RESEARCH ARTICLE

Study of TEC Depletion during Low Solar Activity Periods of 23rd and 24th Solar Cycle at Crest of Indian EIA Region

Surabhi Sahu[1], Richa Trivedi[2*], Amit Jain[3], Sudhir Jain[4]

[1, 3, 4] Institute for Excellence in Higher Education (IEHE), Bhopal, India
[2] University Institutes of Technology, RGPV, Bhopal, India

ABSTRACT: The Total Electron Content (TEC) depletion near the equatorial ionization anomaly crest region in the Indian ionospheric sector has been analyzed during the year March 2005 to February 2006, and May 2016 to August 2017, low solar activity periods of 23rd and 24th solar cycle respectively. TEC data from March 2005 to February 2006 is recorded by GPS Ionospheric Scintillation and TEC Monitor (GISTM) GSV4004A and data from May 2016 to August 2017 is obtained from a multi-frequency multi-constellation Global Navigation Satellite System (GNSS) receiver installed at Bhopal (23.2˚ N, 77.4˚E & MLAT 14.8˚N). TEC depletions have long been recognized as one of the most prominent concerns of space weather as they produce intense scintillation in trans-ionospheric satellite radio signals. All the TEC depletion in the present study occurred in pre-midnight hours and they are more frequent in equinox months during both solar cycles. Among all the events, the severe depletion in TEC was observed on magnetically disturbed day i.e. on 25 October 2016 which may be due to the occurrence of plasma bubble. From ~2 to ~43 TECU and ~5 to ~20 TECU depletions has been detected for the satellite passes along the line of sight of the signal for low solar activity period of 24th and 23rd solar cycle respectively. TEC depletions also show good correspondence with the occurrence of scintillation patches. Rate of change of TEC Index (ROTI) measurements are used to predict the presence of scintillation causing irregularities and its values show the strength of irregularity. Losses of lock were also detected during the encounter of the irregularity when the depletion in TEC is greater than 5 TECU. Results are discussed in terms of possible source mechanism responsible for the occurrence of plasma density depletion.

KEYWORDS: Equatorial ionization anomaly (EIA), Total Electron Content (TEC), TEC depletion, Scintillation, Global Positioning System (GPS).

https://doi.org/10.29294/IJASE.9.4.2023.3033-3046 **©2023 Mahendrapublications.com, All rights reserved**

INTRODUCTION

The depletions in the plasma density are the irregularities of largest scale sizes, wherein the plasma density may be lowered up to two to three orders of magnitude compared to the background content [1]. These depletions rise in altitude from the geomagnetic equator and are seen up to ±15˚ magnetic latitude. The irregularities which occur in form of plasma depletions have scale sizes ranging from centimeters to kilometers. Their duration can vary between minutes to several hours. The irregularities are formed due to gravitational Rayleigh-Taylor (RT) instability processes operating on the steep upward gradient in the bottom side F-region [2,3]. Ionospheric plasma density irregularities are major obstacle to radio wave communication as they result in scattering of radio waves at all frequencies. This leads to the rapid fluctuation of the amplitude and phase of the RF signal known as ionospheric scintillation [4,5]. Due to amplitude scintillation the radio signals fade below the average level. When the depth of fading exceeds from the fade margin of a receiver, the loss of signal and cycle slip are encountered. Phase scintillation leads to frequency shift and when the shift exceeds the phase locked loop bandwidth, the signal is lost and the receiver spends maximum time requiring the signal. Overall, the performance of communication and navigation systems is degraded in presence of amplitude and phase scintillation [6]. Kintner et al., [7] observed that during strong scintillation events, deep amplitude fades may cause signal

**Corresponding Author: richa_trived@yahoo.com*
Received: 05.03.2023 **Accepted:** 17.04.2023 **Published on**: 22.05.2023

disruptions in the receiver-satellite link. The degree to which the ionospheric plasma density irregularities produce scintillation depends on the strength of the irregularities [8]. Understanding the favorable conditions for their onset, growth and persistence are thus of most important in addition to the physical processes leading to the generation of these irregularities in the ionosphere.

It is known that near sunset, the equatorial anomaly begins to weaken due to decrease in plasma densities and dynamo electric field in the E-region. After sunset the polarization charges within the conductivity gradient enhance the eastward electric field, which moves the ionospheric plasma upward allowing the equatorial anomaly crest to intensify. These polarization fields drive F-layer upwards. Later, when electric field turns westward, plasma drifts downward and results in the loss of plasma due to recombination. However, the polarization field is much enhanced just before the reversal time of sunset. This is called the pre-reversal enhancement of eastward electric field [9], which holds the key to the formation of these plasma density irregularities. Farley et al.,[10] first explained the pre-reversal enhancement. The post-sunset eastward electric fields enhance the R-T instability, while westward field quench it and these irregularities can grow to become large ionospheric depletion, frequently called Equatorial Plasma Bubbles (EPBs) [11,12]. In the past years various characteristics of plasma density depletions have been extensively studied using different techniques, like VHF radars [13], rockets [14], ionosondes [15], optical images [16-19], GNSS receivers and satellites [20,21,22]. It is known that the occurrence characteristics of plasma depletions depend strongly on season, longitude sector and solar activity [23,24]. Seemala and Valladares [25] presented the result of diurnal and seasonal variation of GPS-TEC depletion over South American continent for the year 2008, a year of low solar activity. The rate of occurrence, time, duration and the dependence of TEC depletion on local time and season were analyzed at global scale within the latitude belt from 35°N to 35°S for descending phase of solar cycle 23 and ascending phase of solar cycle 24, 2002-2014 [26].

Previous studies [27,28] have investigated the scintillation activity and plasma density depletion dependence on local time, season, longitude, latitude, solar cycle and magnetic activity. The depletion in TEC associated with VHF scintillations at 137 MHz recorded at Arequipa (16.4°N, 71.5°W), Peru during the solar maximum period (1979-1980) have found to have an amplitude less than 5 TEC units and sometimes depletion with amplitude as large as 20 TEC units [29]. Rao et al., [30] studied the spatial and temporal characteristics of trans-ionospheric scintillation for low solar activity period from Jan 2004 to July 2005 at different locations of India. They found that intensity of scintillation activity was stronger around the Equatorial Ionization Anomaly (EIA) region because of increased electron densities and the presence of large gradients which contributes to the occurrence of strong scintillation. Recent observations [4,5,31] using GPS satellites in the equatorial anomaly region, have revealed the occurrence of UHF scintillation and fluctuation in the total electron content in the low latitude Indian ionospheric sector. They noted that there was a one-to-one correspondence between the TEC depletion and increase in S_4 index, whereas enhancements in TEC were completely devoid of increase in S_4. They concluded that the plasma density depletions were the manifestation of plasma bubbles. Sahu et al., [32] studied nighttime enhancements in the VTEC at anomaly crest region and found that very few of the nighttime enhancements occurred with scintillation activity.

Dandekar and Groves [2] studied the occurrence of VHF scintillation and fluctuations in the Total Electron Content (TEC) in the equatorial and low latitude using GPS satellite. Around ±15° of the magnetic latitude, the TEC values are known to be highest. So any fluctuation in TEC at these latitudes results in severe scintillation. In this study we have used GPS satellite measurements at Bhopal, which is at the heart of the equatorial anomaly region in the Indian ionospheric sector, to study the characteristics variability in the TEC and ionospheric scintillation at the anomaly crest region. We present the events of TEC depletion occurred in the EIA region for the period from March 2005 to February 2006 and May 2016 to August 2017, which represent low solar activity periods of solar cycles 23 and 24 respectively.

DATA AND METHOD OF ANALYSIS

Total Electron Content (TEC) and amplitude scintillation (S_4) data from May 2016 to August 2017, recorded by multi-frequency Global

Navigation Satellite System (GNSS) receiver installed at Govt. Maharani Laxmi Bai Girl's P. G. Autonomous College, Bhopal (23.2˚N, 77.4˚E and MLAT 14.2˚N) with the collaboration of Space Physics Laboratory, Vikram Sarabhai Space Centre (SPL, VSSC), Thiruvananthapuram to study the ionospheric irregularities over a station near the crest of equatorial ionization anomaly under In SWIM program. The installed PolaRxS receiver can track up to 32 GPS C/A-code signals, GLONASS and GALILEO signals at L1 (1575.42 MHz), L2 (1227.60 MHz) and L5 (1176.45 MHz) frequency. The data is recorded at one-minute intervals which include TEC, amplitude and phase scintillation along with satellite PRN, azimuthal angle and elevation angle for each satellite tracked by the receiver. The TEC data from March 2005 to February 2006 is obtained by GPS Ionospheric Scintillation and TEC Monitor (GISTM) GSV4004A installed at Bhopal. GISTM system consists of NovAtel OEM4 dual frequency GPS receiver and a low phase noise oven-controlled crystal oscillator (OCXO) that is required for monitoring phase scintillation.

Amplitude scintillation is defined as the standard deviation of the received signal power normalized to average signal power. As the S_4 index is affected by ambient noise, two indices are recorded by the receiver namely, total S_4 $(S_4)_{tot}$ and correction to S_4 $(S_4)_{corr}$. The corrected S_4 is then calculated as follows:

$$S_4 = \sqrt{(S_4)^2_{tot} - (S_4)^2_{corr}} \quad (1)$$

In this study, we defined weak scintillation as S_4 between 0.2 and 0.6 and strong scintillation as S_4> 0.6 and neglected the scintillation below 0.2.

The phase and group velocities of signals from the satellite are affected due to variations in the TEC. The total number of free electrons in a column of 1 m^2 cross-section along the path of electromagnetic wave between the satellite and the receiver is called Slant Total Electron Content (STEC) or simply TEC measured in TECU, where 1 TECU= 10^{16} electrons m^{-2}. STEC is obtained from the difference between the phases L1 and L2 of the two GPS signals [33,34] as:

$$STEC = \frac{1}{40.3} \times \left[\frac{1}{L_1^2} - \frac{1}{L_2^2}\right]^{-1} \times (P_1 - P_2) + TEC_{CAL} \quad (2)$$

where, P_1= Pseudo range at L_1 and P_2= Pseudo range at L_2 in meters. TEC_{CAL} represents the bias correction which depends on the satellite-receiver pair.

Pi et al., [35] monitored the global ionospheric irregularities by using worldwide GPS network and they showed that the Rate of TEC Index (ROTI) can be used as a parameter to identify the small-scale density fluctuations to study the ionospheric irregularities. They defined ROTI based on the standard deviation of Rate of TEC (ROT) as follows:

$$ROTI = \sqrt{\overline{ROT^2} - \overline{ROT}^2} \quad (3)$$

where, $ROT = \frac{\Delta STEC}{\Delta t}$ and show the average value.

STEC represents the TEC along the ray path from the satellite to the receiver and Δt denotes the sampling interval in seconds.

Due to depletion in TEC, we generally observe that there is an abrupt change in the ROTI value and corresponding increase in the corrected scintillation (S_4). We have considered only those events for which depletion in TEC occurred above 20˚ elevation angle in order to minimize multipath effects. To discuss and present the observed data we have drawn - four panels in Fig. 1,3, 4, 6, 7, 9, 10, 11 and 12 along with the satellite loss of lock for all the events. Panel A represents geomagnetic latitude (left y-axis) and geographic longitude (right y-axis) in degrees of Ionospheric Pierce Point (IPP), panel B represents the satellite elevation angle (in degrees), panel C shows the Rate of TEC Index (ROTI in TECU/5 minute or TECU/ 2 minute) and panel D gives the variation in slant TEC or STEC in TECU (left y-axis) and corrected S_4 (right y-axis).The horizontal line in panel B shows the cut-off elevation at 20˚. Geomagnetic latitude and geographic longitude are the latitude and longitude of IPP assuming a thin ionospheric shell at an altitude of 350 km in the Line of Sight (LOS) between GPS receiver and the satellite. This has been computed in post processing of the data.

RESULTS AND DISCUSSION

A. TEC depletions for low solar activity period of solar cycle 24 (2016-2017)

A.I. 23 May 2016

The irregularity in terms of TEC depletion and scintillation were recorded by the GNSS

receiver at Bhopal on 23 May 2016 from 1237 to 1241 hrs UT along five satellite paths (GPS-PRN#17, #19; GLONASS-PRN#43, #58; GALILEO-PRN#78). In all PRNs the depletion in the TEC ranges from 1.5 to 12 TECU along with scintillation (S_4) rises up to 1.01 units. The range of IPP latitude and longitude were ~26.81°N to 18.26°N and ~84.14°E to 79.5°E respectively with variation in MLAT from 9.47°N to 18.24°N. Among all reported PRNs more significant variation were observed in PRN #17 on 23 May 2016, hence selected for this study.

Fig. 1 gives the ionospheric observations for PRN #17 on 23 May 2016. The geomagnetic latitude and longitude of IPP for PRN #17 is plotted (panel A). The curve drawn with thick solid line represents MLAT and thin line curve represents longitude of IPP. The satellite is observable from about 11° above the horizon and its highest elevation is about 69° with respect to the site of observation (panel B). The satellite goes below the horizon just after 1344 hrs UT. The variation of ROTI shows the strength of irregularity observed in PRN #17 (panel C). A sudden depletion is observed in TEC around 1237 hrs UT and this region has been highlighted by two vertical lines marked with **a** and **b**. Depletion in TEC has been reduced by about 12 units and corrected S_4 enhanced to 1.017 units coinciding with the occurrence of TEC depletion. The satellite elevation angle is ~24° at this hour. The steep change in ROTI from ~1 to ~3 units show that the irregularity strength was very intense and confirmed by the sharp depletion in TEC and increased S_4 to a larger extent. The depletion in TEC recovered very fast when the geomagnetic latitude and longitude of IPP was almost constant, about 16°N and 83°E respectively. The lock time of PRN #17 for 23 May 2016 is shown in Fig. 1 (Right). It is clear from the Fig. that during the encounter of irregularity there was loss of lock detected in L2 signal which degrades the signal strength. On the same day higher scintillation and slight TEC depletion were recorded by the receiver from 1309 hrs UT to 1317 hrs UT in all five satellite paths. Significant TEC depletion of ~3.76 TECU in PRN#19 and ~2.3 TECU in PRN#58 were also observed.

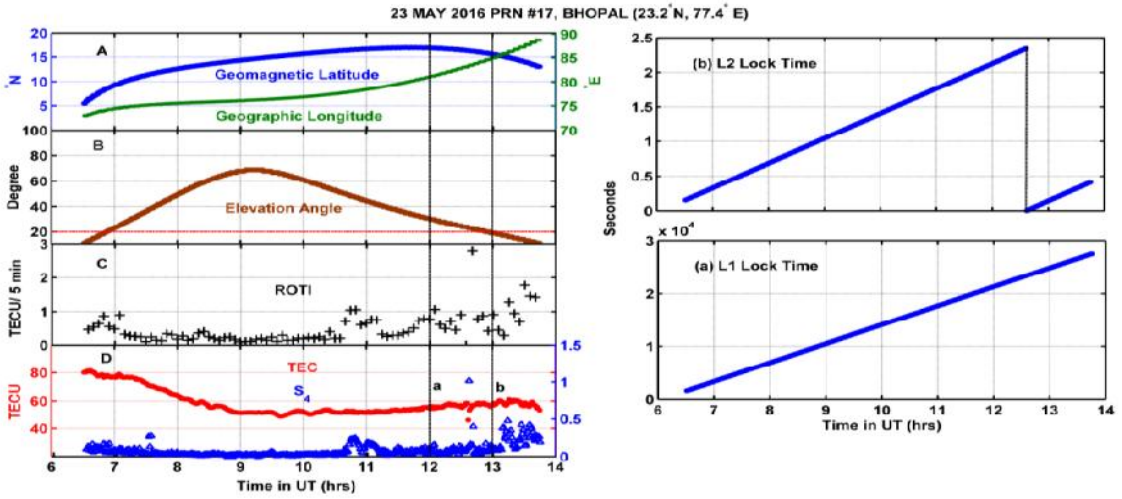

FIG. 1: TEC depletion observed on 23 May 2016 for PRN #17. Panel A gives the variation of MLAT (Left y-axis) and Geographic longitude (Right y-axis) of the Ionospheric Pierce Point (IPP). Panel B gives the satellite elevation angle in degrees (Red line parallel to x-axis gives the elevation cut off at 20°). Panel C gives the Rate of TEC Index (ROTI) and Panel D gives the variation in slant TEC or STEC (Left y-axis) and S_4 Index (Right y-axis). The horizontal axis in each panel gives the Universal Time (UT). L1 and L2 Lock Time are also shown for PRN #17 (Right).

The contours of the amplitude scintillation (S_4) can be seen in the Fig. 2 for 23 May 2016 and we have also considered an earlier day i.e., 22 May 2016 to show the difference in scintillation activity. The figure clearly shows that one major region (~13°N MLAT) and 04 very small regions of higher S_4 (MLAT ~9.5°N, ~14°N, ~16°N and ~18°N) observed between 1230 to 1240 hrs UT. Similar region of higher and moderate S_4 were also seen during 1305 to 1317 hrs UT, whereas no scintillation activity was present on 22 May 2016.

A.II. 09 October 2016

Another result of TEC depletion observed on 09 October 2016 in PRN #16 (GPS) and PRN#48 (GLONASS) is shown in Fig. 3 and 4 (Left)**.** The highest elevation angle attained by the PRN #16 is about 73˚ (panel B) and latitudinal extent of IPP for the entire series of depletion is from 6˚N to 12˚N (MLAT). The TEC variation shows a series of well-defined depletions between 1500 and 16000 hrs UT, which is highlighted with two vertical lines **a** and **b**. This region is embedded with a number of separated TEC depletions with maximum depletion up to ~20 TECU and in correspondence S_4 reaches to 1.047 units (panel D). The corrected S_4 shows dependence with the occurrence of depletion in TEC. It can be seen from panel C of Fig. 3, that ROTI (~6 TECU/ 5 min) shows significant variation during the time of multiple depletions. Similar to PRN #16 the depletion in TEC of about 38 TECU was detected in PRN #48 around 1516 hrs UT as shown in Fig. 4. Due to the strong enhancement in scintillation activity, losses of lock were observed in L2 in both the satellites signals as shown in Fig. 3 and 4 (Right) for PRN #16 and PRN #48 respectively.

The contours of Amplitude Scintillation (S_4) for 08 and 09 October 2016 are plotted in Fig. 5 for all visible satellites between 1500 to 1600 hrs UT. The Figure clearly shows that due to TEC depletion, strong and moderate irregularity region is observed (MLAT ~8˚N to 11˚N) between 1515 to 1600 hrs UT on 09 October 2016 while no scintillation activity is seen on comparing day i.e.,08 October 2016.

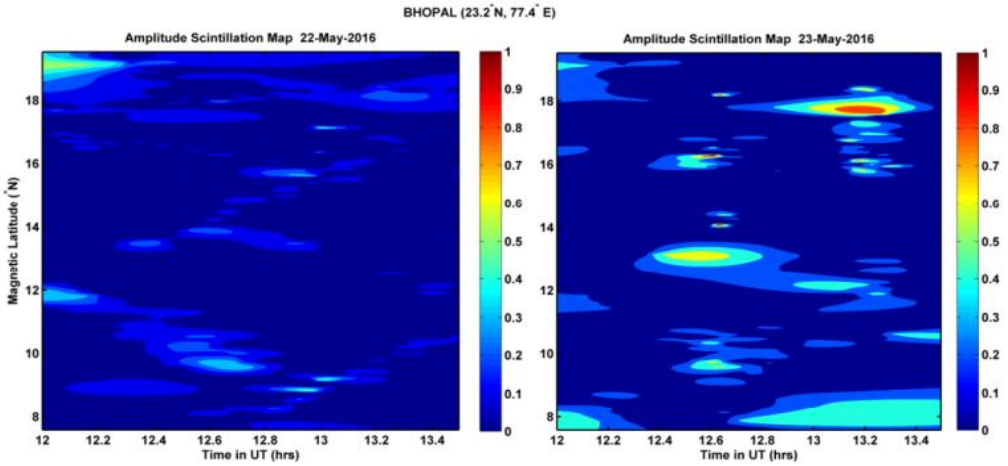

FIG. 2: S_4 Contours for all visible satellites between 1200 to 1330 hrs UT for 22 May 2016 (Left) and 23 May 2016 (Right)

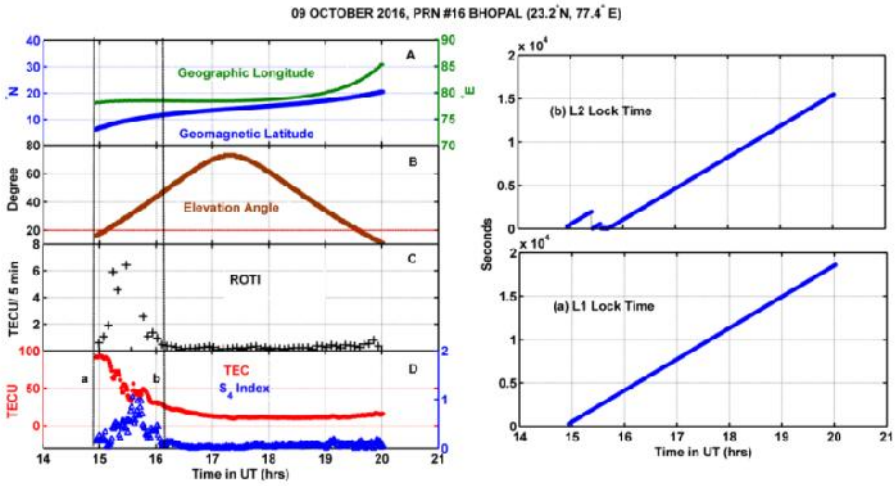

FIG. 3: Same as Fig. 1 but for 9 October 2016 for PRN #16 (GPS).

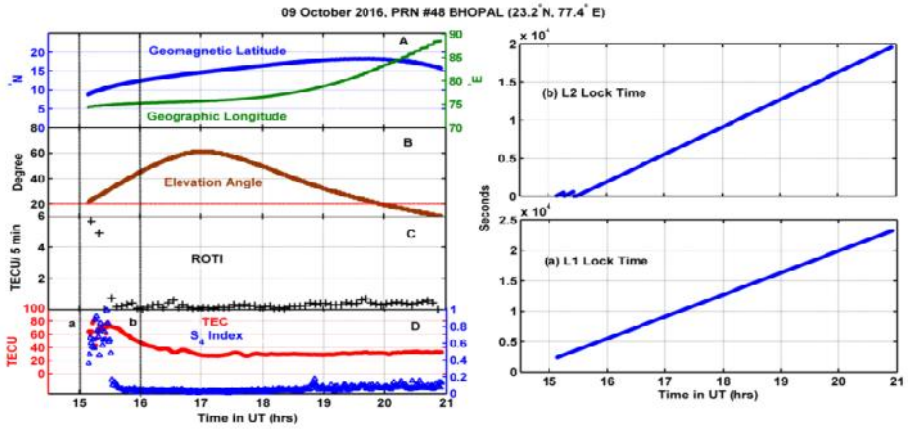

FIG. 4: Same as Fig. 1 but for 9 October 2016 for PRN #48 (GLONASS).

A.III. 25 October 2016

The depletion in TEC observed on 25 October 2016 in PRNs #10 and #16 are shown in Fig. 6 and Fig. 7 respectively. The highest elevation angle attained by the PRN #10 is around 55° (panel B). In the depleted region, the geomagnetic latitude of IPP varies from 12.14°N to 7.1°N and longitude was almost constant ~81°E (panel A). The TEC values vary with increase in satellite elevation angle and two consecutive TEC depletions are observed at 1348 and 1430 hrs UT, where the TEC value decreased by about 43 TECU and 30 TECU respectively (panel D). This region has been highlighted by two vertical lines marked by **a** and **b**. The ROTI steeps to 10 TECU/5 min (panel C) during this period, showing the strength of the irregularity. At the time of consecutive depletions, the corrected S_4 is observed around 1.169 and 1.058 respectively. The lock time for PRN #10 is shown in Fig. 6 (Right). For PRN #16 (Fig. 7 (Left)) the range of geomagnetic latitude is quite wide and varies from 4°N to 20°N, its longitude also varies from 77°E to 85°E for the entire pass of the PRN #16 (panel A). An interpolation of TEC between the region **a** and **b**, imply that the whole region is embedded with number of depletions (panel D). Beyond the line **b** the TEC is smooth and S_4 reaches at noise level. Owing to the satellites' trajectory, the latitudinal extent of IPP for the region **a** and **b** varies from 8°N to 11°N but the geographic longitude remains almost constant (~78°E). It helps us to identify that these depletions are nearly field aligned. A number of depletions can be observed in the elevation range 20° to 45° in panel B of the Figure. The corrected S_4 and ROTI show dependence on the occurrence of depletions in TEC. Due to this significant scintillation activity, losses of lock occurred in L1 twice and on L2 more than two occasions in PRN #16 as shown in Fig. 7 (Right).The enhanced ROTI values (~10 TECU/5 min) and strong scintillation (>1.0) along with multiple occurrences of losses of lock in both the PRNs confirmed severity of the irregularity which seems to be plasma bubble.

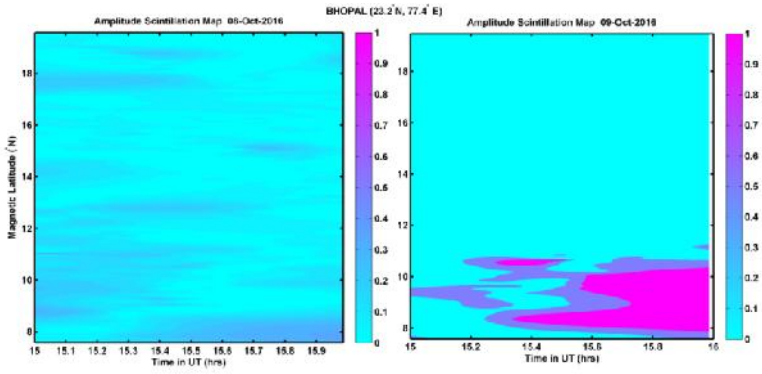

FIG. 5: S_4 contours for all visible satellites between 1500 and 1600 hrs UT for 08 Oct 2016 (Left) and 09 October 2016 (Right)

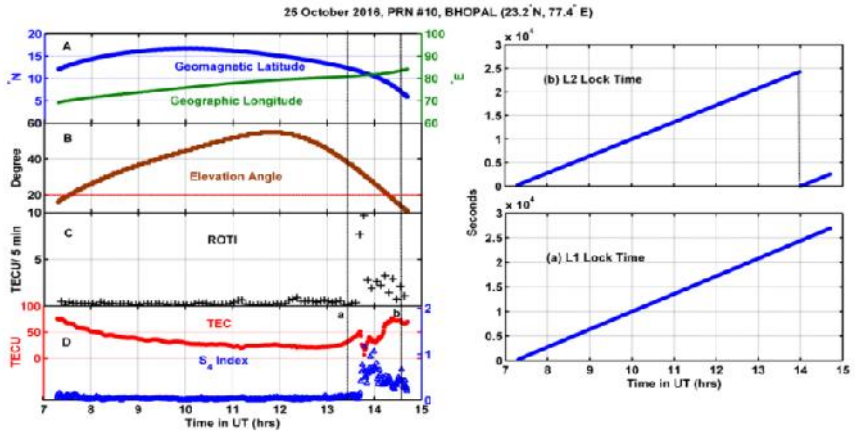

FIG. 6: Same as Fig. 1 but for 25 October 2016 for PRN #10 (GPS)

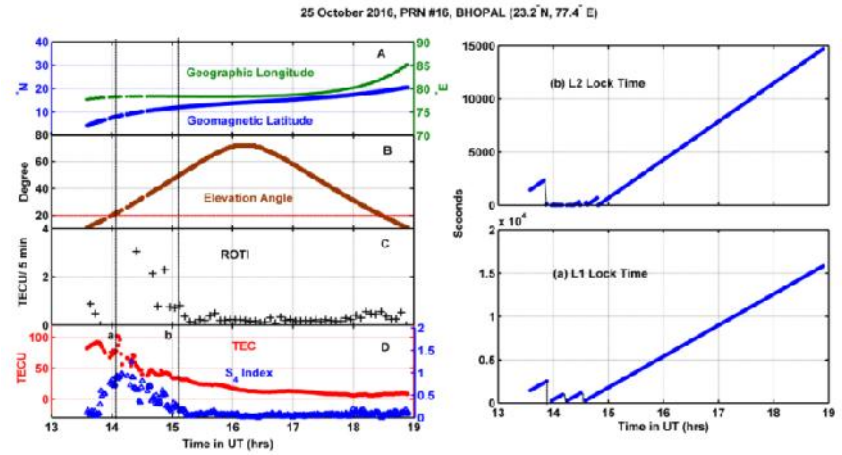

FIG. 7: Same as Fig. 1 but for 25 October 2016 for PRN #16 (GPS).

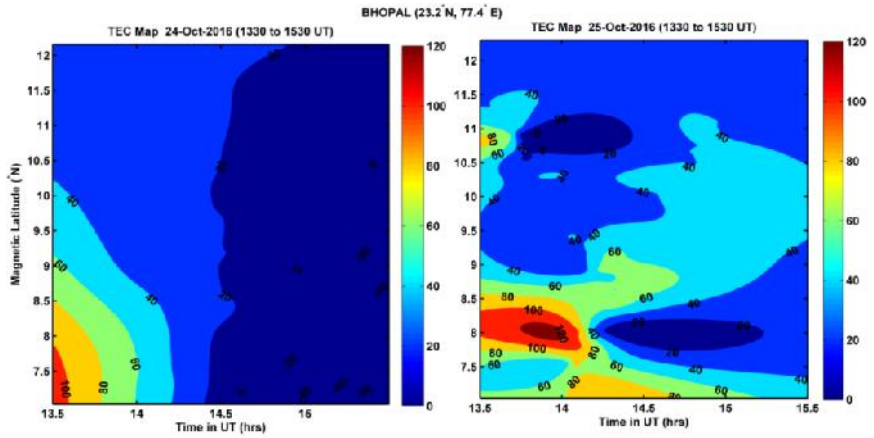

FIG. 8: TEC Map for PRN #10 & #16 for 24 October 2016 (Left) and 25 October 2016 (Right) (Grid: GMLAT [.01°] × UT [1 min])

The contours map of TEC for 24 and 25 October 2016 is shown in Fig. 8. The low density TEC region occurred around 1343 to 1418 hrs UT (MLAT ~11.5°N) on 25 October 2016, while no such region can be seen on 24 October 2016, a

comparison day and shows a normal variation pattern.

B. TEC depletions for low solar activity period of solar cycle 23 (2005-2006)

The study of TEC depletion for the low solar activity period from March 2005 to February 2006 for Bhopal using GPS TEC data has been carried out. A total 6 depletions in TEC were observed during the period and out of these, 3 most significant events considered and used to compare with the results of low solar activity of 24th solar cycle.

B.I. 16 March 2005

The irregularity in terms of TEC depletion observed on 16 March 2005 in PRN #16 is shown in Fig. 9.The highest elevation angle attained by the satellite is about 66° as seen from panel B. The high ROTI value shows the strength of the irregularity observed in PRN #16 (panel C). A steep change in ROTI (0.8/ 2 min) and sudden reduction in TEC of about 20 TECU is observed at 1540 hrs UT. Coinciding with the time of occurrence of depletion, corrected S_4 suddenly shoots up to 0.5 units (panel D) which confirm the event. During the encounter of the irregularity, the MLAT of IPP varies from 8°N to 11°N while the longitude is nearly constant around 78°E (panel A). The depletion in TEC last for 42 minutes, thereafter the variations in TEC are smooth and S_4 reaches at its noise level.

The lock time for PRN #16 is shown in Fig. 9 (Right). During the passes of the irregularity, the loss of lock in L1 and L2 occurs more than twice, which degrades the signal strength. It implies a sudden loss of phase lock of the signal due to increases scintillation activity.

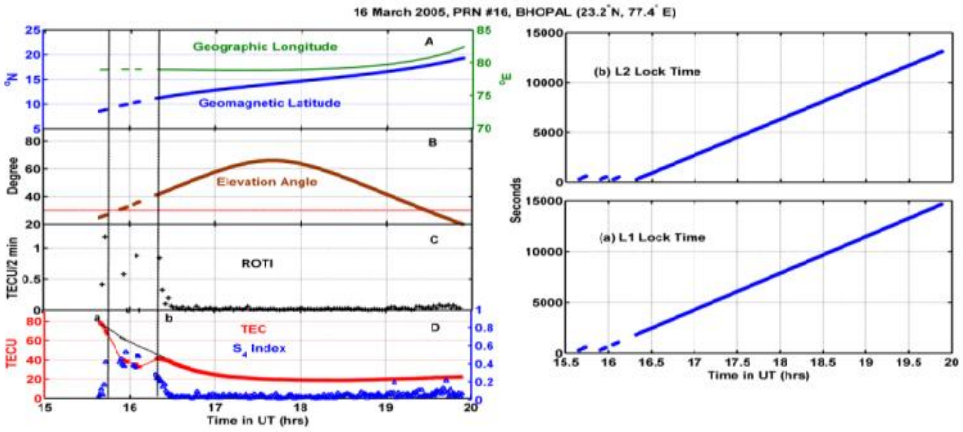

FIG. 9: Same as Fig. 1 but for 16 March 2005 for PRN #16.

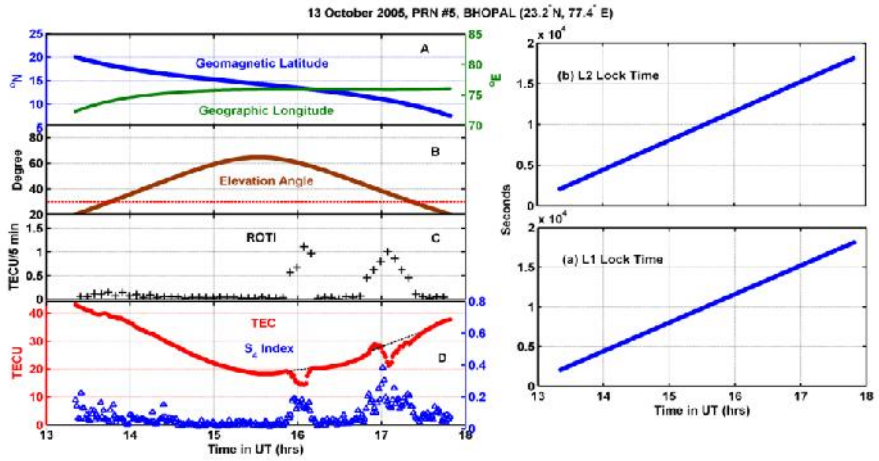

FIG. 10: Same as Fig. 1 but for 13 October 2005 for PRN #5.

B.II. 13 October 2005

Depletion occurred on 13 October 2005 is presented in Fig. 10 for PRN #5. As is evident from Figure, the satellite attains a very high elevation of about 65˚ (panel B). Two consecutive sets of TEC depletion (5 TECU) are observed around 1555 and 1700 hrs UT respectively. Corresponding to TEC depletion there is significant sudden increase in scintillation and ROTI values (panel C). Between two depletions, the TEC variation is smooth and corrected S_4 reaches is at lowest noise level (panel D). The latitudinal extent of IPP for the two sets of depletions is around 14˚N and 10˚N respectively but the geographic longitude remains constant (76˚E) which implies that the satellite is moving along the geographic meridian (panel A). The first depletion region is seen at higher elevation range (62˚ to 59˚), as compared to second (45˚ to 30˚). There is no loss of lock detected in the satellite signal as shown in Fig. 10 (Right).

B.III. 31 October 2005

Depletion in TEC recorded by PRN #29 and #30 on 31 October 2005 and their respective observations are shown in Fig. 11 and 12.

Fig. 11 reflects that PRN #29 attained the highest elevation angle around 45˚ (panel B) and the satellite traversed the same longitude for most of its pass. In point of fact, almost all GPS satellites have a very slow east-west motion. Thus, these satellites offer an opportunity to observe along the same field lines. Initially when the PRN #29 locked at 1515 hrs UT, it experiences loss of lock in L1 and L2 twice and after that there is depletion in TEC of about 8 TECU (panel D). The depletion in TEC last up to 1600 hrs UT and thereafter the TEC variation is smooth and recovered to its normal value. The latitudinal extent of IPP for the depleted region is from 9˚N to 12˚N (MLAT) but the geographic longitude is almost constant, and it is around 81˚E (panel A). The satellite is nearly overhead at this hour, as revealed from the elevation (~36˚). The steep change in ROTI value (~1 TECU) shows the strength of the irregularity (panel C) which is confirmed by the sudden depletion in TEC and increased corrected S_4 (0.4).

Fig. 12 shows the observations for PRN #30 on 31 October 2005. The results are very informative as depletion in PRN #30 appears about an hour after PRN #29, and the maximum elevation angle for PRN #30 is about 6˚ higher than for PRN #29 (panel B). PRN #30 detects the irregularity around 1630 hrs UT. The depletion in TEC (around 8 Units) occurred between 1630 to 1712 hrs UT (panel D). The latitudinal extent of IPP for the depleted region varied from 11˚N to 8˚N, while the longitude is almost constant around ~74˚E (panel A). The depletion in TEC is well correlated with the increased scintillation and steep change in ROTI ~1.8 TECU/2 min (panel C).The lock time for PRN #29 and PRN #30 is shown in Fig. 11 (Right) and Fig. 12 (Right) respectively. It is clear from the Figures that loss of lock in L1 and L2 occurs in both the satellite signal due to enhanced scintillation activity.

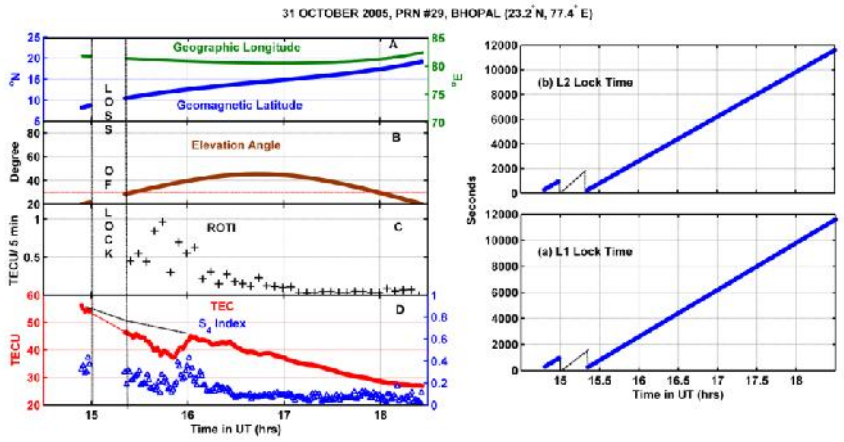

FIG. 11: Same as Fig. 1 but for 31 October 2005 for PRN #29.

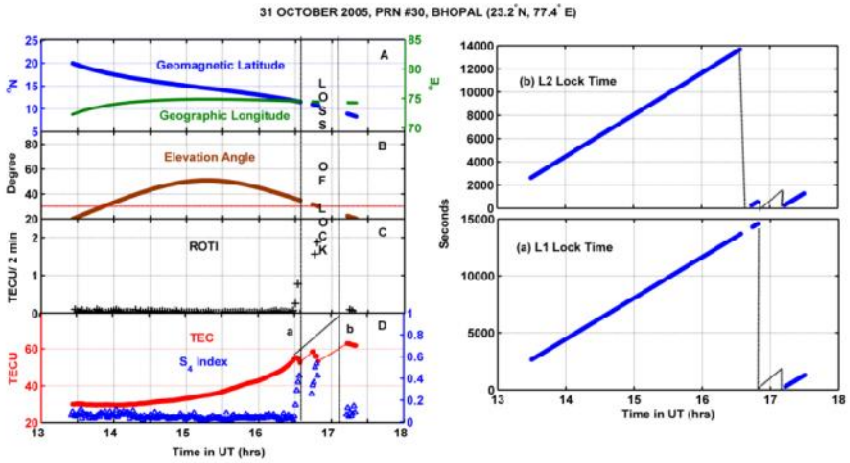

FIG. 12: Same as Fig. 1 but for 31 October 2005 for PRN #30.

The plasma density depletions are generated at the bottom side of the equatorial F region and move to the top side. Since the electron density of the F region contributes greatly to the TEC values, any variation in the density of F region would be reflected in the TEC.[36] Sudden TEC reduction in the equatorial region is generally identified as the plasma density depletion in the F region of the ionosphere.[4]Consistent with this, the depletion in TEC (~2 to ~43 TECU) reported in Fig. 1 through 12 have been identified as manifestation of plasma bubble of equatorial origin. Small scale irregularities, associated with these depletions, manifest an increase in corrected S_4 when the depleted ionospheric plasma comes in to the line-of-sight between the GPS satellite and the receiver. In the present study, small-scale irregularities are associated with TEC depletion and are responsible for scintillation and high ROTI values. The large TEC depletion observed on 9 and 25 October 2016 and 16 March and 31 October 2005 seems to be plasma bubble events since the irregularity strength was very intense and multiple losses of lock occurred along with scintillation and high ROTI values. Similar cases of TEC depletion were reported by Rao et al.,[37]over Indian EIA region Udaipur and near equatorial station Bengaluru. The plasma density depletions, also known as equatorial plasma bubbles (EPB), are the phenomena which occurs during post-sunset period in the equatorial F-region. The presence of these TEC depletions causes' turbulent ionospheric conditions that disrupt the satellite based communication and navigation system.

During the post-sunset period, the F-region of the equatorial ionosphere often becomes unstable through a complex interaction between electric fields, neutral winds and the Earth's magnetic field [38]. The enhancement in the post-sunset upward plasma drift is believed to be the chief constituent in the generation of Equatorial Spread-F [39]. During the day-time the vertical polarization electric field, setup by the dynamo currents at ionospheric F-region altitudes, are short circuited through the conductivity in the sunlit E-layer to the north and south of magnetic equator. After sun-set, the F-region dynamo starts to dominate. The strengthening of the electric field is caused by this influence of the dynamo in the F region in conjunction with the conductivity gradient across the solar terminator. The eastward electric field, associated with the F-region dynamo, gets enhanced following the decrease in the E-region conductivity. This field induces the upward **E×B** drift. This pre-reversal enhancement of the eastward electric field raises the F layer plasma to high altitudes. The plasma lifted until pressure gradients are large enough to diffuse in to the tropics along the magnetic field lines. At these altitudes, recombination is slow, so regions of enhanced density persist after midnight forming equatorial anomaly at ±15° from the magnetic equator. Also, lower ionosphere rapidly decays after sunset due to the rapid recombination of electrons and ions forming a steep gradient at the base of the F-region. This creates favorable conditions for a gravitational Rayleigh-Taylor instability. The non-linear development of these instabilities leads to the formation of plasma depleted regions called bubbles [27,40].Within the bubbles, the polarization electric field is higher and as a result, the bubbles rise to the

topside at a higher velocity than ambient plasma drift [41]. As the bubble rise to higher heights, the steep gradient on the edges of depletion generates small-scale irregularities [42]; widely recognized as plumes in a radar backscatter map.

In order to see the dependence on solar activity, a comparative study of TEC depletion events for low solar activity period of 23rd and 24th solar cycle have been carried out. Most of the events occurred during equinox month and mainly in the pre-midnight hours similar to the results of Kumar et al.,[43]. The alignment of solar terminator with the magnetic meridian in two hemispheres plays an important role in producing maximum occurrence of plasma density depletions during equinox season [44]. In addition, in the longitudinal sectors where there is strong declination, EPBs can occur, for example, during the summer [45]. The alignment between the solar terminator and magnetic meridian becomes closer, in equinox seasons, which causes the reduction in E region conductivity. The reduction E region conductivity is responsible for producing the **E×B** plasma drift in the equatorial F layer. This plasma drift in the equatorial F layer creates a favorable situation for the formation of these irregularities during the equinox season.

The strong level of amplitude scintillation causes the received signal power to drop below the receiver's threshold limit and loss of lock is observed [30]. Losses of lock were also detected for all the events reported in the present study when depletion in TEC was greater than 5 TECU. It is observed that L1 tracking performance was degraded to a lesser extent than L2. So, we can conclude that loss of lock of signal depends on the magnitude of the irregularity. It was also observed that the receiver loses its lock more than once as shown in Figure 7, 9, 11 and 12. These depletions in TEC have been identified as a manifestation of the plasma density depletions of the equatorial origin [46].

Plasma density depletions are of particular importance when they extend to the latitudes of anomaly crest regions. At these regions, the irregularities intersect the highest level of electron density. So the radio frequency signals propagating through this intersection undergoes the highest disruptive levels of scintillation both in amplitude and phase [47]. This is the reason that increase in the corrected S_4 are seen at the same time when depletion in TEC is observed for all the events reported here as well as reported by Yeh et al.,[48]. When the TEC depletions extend in latitude to the anomaly crest regions, the strong scintillation, which are associated with these small-scale irregularities degrade the positional accuracy in the satellite navigational systems such as GPS [30].

CONCLUSION

The study of TEC depletion at anomaly crest region Bhopal have been analyzed during the year March 2005 to February 2006 and May 2016 to August 2017, low solar activity periods of 23rd and 24th solar cycle. All the TEC depletion observed in the present study occurred during pre-midnight hours due to post sunset enhancement of eastward electric field. Most of the depletion observed in equinox months for both solar cycles.TEC depletions from ~2 to ~43 TECU were observed between 8°N to 18°N (MLAT) and ~5 to 20 TECU between 9°N to 14°N for low solar activity period of 24th and 23rd solar cycle respectively. A total of 6 TEC depletions were observed during the observation period in which the large TEC depletion observed on 9 and 25 October 2016 and 16 March and 31 October 2005 seems to be plasma bubbles events since the irregularity strength was very intense and multiple losses of lock occurred. Along with losses of lock, the corrected S_4 and ROTI value reaches up to 1.242 and 9.68 TECU/5 min for 24th solar cycle and 0.5 and 2 TECU/5 min for 23rd solar cycle respectively. In the present events, losses of lock of GPS signals occurred only when depletion in TEC was greater than 5 TECU due to strong level of amplitude scintillation.

ACKNOWLEDGEMENTS

This work is supported by the Indian Space Research Organization (ISRO). The GPS data of 2016 have been collected as a part of the Space weather programme (InSWIM) of the Space Physics Laboratory (SPL), Vikram Sarabhai Space Center, Thiruvananthapuram. These data are the property of ISRO and can be made available on request to Raj Kumar Choudhary (rajkumar_choudhary@vssc.gov.in). Authors are thankful to SPL VSSC Thiruvananthapuram for installation of GPS receiver at Bhopal. Solar flux (F10.7 cm) and Ap index data are downloaded from (http://omniweb.gsfc.nasa.gov/form/dx1.html).

REFRENCES

[1] Hanson W.B. and Sanatani S, 1973. Large Ni gradients below the equatorial F peak, J. Geophys. Res. 78(7), 1167-1173

[2] Dandekar B.S., Groves K. M., 2004. Using ionospheric scintillation observations for studying the morphology of equatorial ionospheric bubbles, Radio Science. 39, RS3010.

[3] Magdaleno S.M., Herraiz M., Altadill D., Morena B.A., 2017. Climatology characterization of equatorial plasma bubbles using GPS data, J. Space Weather Space Clim. 7, A3.

[4] Dashora N. and Pandey R. , 2005. Observations in equatorial anomaly region of total electron content enhancements and depletions, Ann. Geophys. 23(7), 2449-2456.

[5] Olwendo J.O., Cilliers P.J., Baki P., Mito C., 2012. Using GPS-SCINDA observations to study the correlation between scintillation, total electron content enhancement and depletions over the Kenyan region, Advance in Space Res. 49(9), 1363-1372.

[6] Ray S., Paul A., Das Gupta A.,2006.Equatorial scintillations in relation to the development of ionization anomaly, Ann. Geophys. 24, 1429-1442.

[7] Kintner P.M., Kil H., Beach T.L., dePaula E.R., 2001, Fading Timescales associated with GPS signals and potential consequences, Radio Sci. 36(4), 731-743.

[8] Kintner P.M., Ledvina B.M., de Paula E.R., 2007.GPS and ionospheric scintillations, Space Weather. 5(9), S09003.

[9] Rishbeth H., 1971. Polarization fields produced by winds in the equatorial F-region, Planet Space Sci. 19, 357-369.

[10] Farley D.T., Bonelli E., Fejer B.G., Larse M.F.,1986. The pre reversal enhancement of the zonal electric field in the equatorial ionosphere, J. of Geophys. Res. 91(A12), 13723-13728.

[11] Kelley M.C., Larsen M.F., LaHoz C., McClure J.P., 1981. Gravity wave initiation of equatorial spread-F: A case study,J. Geophys. Res. 86(A11), 9087-9100.

[12] Fejer B.G., Scherliess L., de Paula E.R., 1999.Effects of the vertical plasma drift velocity on the generation and evolution of equatorial spread F, J. Geophys. Res. 104(A9), 19859-19869.

[13] Abdu M.A., Kherani E.A., Batista I.S., de Paula E.R., Fritts D.C., Sobral J.H.,2009. Gravity wave initiation of equatorial spread F/ plasma bubble irregularities based on observational data from the SpreadFEx campaign, Ann. Geophys. 27, 2607-2622.

[14] Muralikrishna P., Vieira L.P., Abdu M.A., 2007. Spectral features of E- and F-region plasma irregularities as observed by rocket borne electron density probes from Brazil," Revista Brasileira de Geofisica. 25, 115-128.

[15] Abdu M.A., Batista I.S., Reinisch B.W., MacDougall J.W., Kherani E.A., Sobral J.H., 2012.Equatorial range spread F echoes from coherent backscatter and irregularity growth processes, from conjugate point digital ionograms,Radio Sci. 47(6), RS6003.

[16] Takahashi H., Taylor M.J., Sobral J.H., Medeiros A.F., Gobbi D., Santana D.C., 2001.Fine structure of the ionospheric plasma bubbles observed by the OI 6300 and 5577 airglow images, Advance in Space Res. 27(6-7), 1189-1194.

[17] Arruda D.C., Sobral J., Abdu M., Castilho V.M., Takahashi H., Medeiros A., Buriti R., 2006.Theoretical and experimental zonal drift velocities of the ionospheric plasma bubbles over the Brazilian region, Advance in Space Res. 38, 2610-2614(2006).

[18] Paulino I., Medeiros A.F., Buriti R.A., Takahashi H., Sobral J.H.A., Gobbi D.,2011. Plasma bubble zonal drift characteristics observed by airglow images over Brazilian tropical region, Revista Brasileria de Geofisica. 29(2), 239-246

[19] Taori A., Patra A.K., Joshi L.M., 2011. Gravity wave seeding of equatorial plasma bubbles: An investigation with simultaneous F region, E region, and middle atmospheric measurements," J. of Geophys Res. 116(A5), A05310.

[20] Rezende L.F.C., dePaula E.R., Kantor I.J., Kintner P.M., 2007. Mapping and survey of plasma bubble over Brazilian territory, J. of Navigation. 60, 69-81.

[21] Huang C.S., de La Beaujardiere, Roddy P.A., Hunton D.E., Ballenthin J.O., Hairston M.R., 2013. Large-scale quasiperiodic plasma bubbles: C/NOFS observations and casual mechanism," J. Geophys. Res. Space Phys. 118(6), 3602-3612.

[22] Park J., Luhr H., Noja M, 2015. Three-dimensional morphology of equatorial plasma bubbles deduced from measurements onboard CHAMP, Ann. Geophys. 33, 129-135.

[23] Aarons J., 1993. The longitudinal morphology of equatorial F-layer irregularities relevant to their occurrence, Space Sci. Rev. 63(3), 209-243.

[24] Huang C.Y., Burke W.J., Machuzak J.S., Gentile L.C., Sultan P.J., 2001. DMSP observations of equatorial plasma bubbles in the topside ionosphere near solar maximum, J. Geophys. Res. 106(A5), 8131-8142.

[25] Seemala G.K. and Valladares C.E., 2011. Statistics of total electron content depletions observed over the South American continent for the year 2008, Radio Sci. 46, RS5019.

[26] Blanch E., Altadill D., Juan J.M., Camps A., Barbosa J., Casado G.G., Riba J., Sanz J., Vazquez G., Perez R.O.,2018. Improved characterization and modeling of equatorial plasma depletions, J. Space Weather Space Clim. 8, A38.

[27] Woodman R.F., LaHoz C., 1976. Radar observations of F region equatorial irregularities,, J. Geophys. Res. 81(31), 5447-5466.

[28] Muella M.T., Paula E.R., Kantor I.J., Rezende L.F.C., Smorigo P.F., 2009. Occurrence and zonal drifts of small scale ionospheric irregularities over an equatorial station during solar maximum-Magnetic quiet and disturbed conditions, Advance in Space Res. 43(12), 1957-1973.

[29] DasGupta A., Basu S., Aarons J, Klobuchar J.A., Basu S., Bushby A.,1983. VHF amplitude scintillations and associated electron content depletions as observed at Arequippa Peru, J. of Atmos. and Terr. Phys. 45(1), 15-26.

[30] Rao P.V.S., Gopi K.S., Niranjan K., Prasad D.S.V.V.D.,2006.Study of spatial and temporal characteristics of L-band scintillations over the Indian low-latitude region and their possible effects on GPS navigation, Ann. Geophys. 24, 1567-1580

[31] D'ujanga F.M., Mubiru J.,Twinamasiko B.F., Basalirwa C., Ssenyonga T.J.,2012, Total electron content variations in equatorial anomaly region, Advance in Space Res. 50(4), 441-449.

[32] Sahu S., Pal A., Choudhary R.K., Jain A., Jain S., 2020. Nighttime enhancements in the VTEC at anomaly crest region Bhopal: Solar and magnetic activity effects," Advance in Space Res. 66(10), 2289-2301.

[33] Jain A., Tiwari S., Jain S., Gwal A.K., 2011, Nighttime enhancement in TEC near the crest of northern equatorial ionization anomaly, Ind. J. Phys. 85(9), 1367-1380.

[34] Trivedi R., Jain S., Jain A., Gwal A.K., 2013. Solar and Magnetic activity control on nighttime enhancement in TEC near the crest of the equatorial ionization anomaly,"Advance in Space Res. 51(1), 61-68.

[35] Pi X., Mannucci A.J., Lindqwister U.J., Ho C.M., 1997.Monitoring of global ionospheric irregularities using the worldwide GPS network, Geophys. Res. Letters 24(18), 2283-2286.

[36] Deng B., Huang J., Liu W., Xu J., Huang L.,2013. GPS scintillation and TEC depletion near the northern crest of equatorial anomaly over South China,Advance in Space Res. 51(3), 356-365.

[37] Rao S.S., Sharma S., Pandey R. 2018, Study of night time TEC depletion over Indian region, Ind. J. of Radio and Space Phys. 47, 5-8.

[38] Rishbeth H., 1981. The F-region dynamo, J. of Atmos. and Terr Phys. 43(5-6), 387-392.

[39] Basu S., Kudeki E., Basu S., Valladares C.E., Weber E.J.,. Zengingonul H.P, Bhattacharyya S., Sheehan R., Mriwether J.W., Biondi M.A., Kuenzler H., Espinoza J.,1996. Scintillations, plasma drifts, and neutral wind in the equatorial ionosphere after sunset, J. Geophys. Res. 101(A12), 26795-26809.

[40] Haase J.S., Dautermann T., Taylor M.J., Chapagain N., Calais E., Pautet D., 2011. Propagation of plasma bubbles observed in Brazil from GPS and airglow data, Advance in Space Res. 47, 1758-1776.

[41] Anderson D.N. and Haerendel G., 1979. The motion of depleted plasma regions in the equatorial ionosphere,J. Geophys. Res. 84, 4251-4256.

[42] Costa E., Kelley M.C., 1978. On the role of steepened structures and drift waves in equatorial spread F, J. Geophy. Res. 83(A9), 4359-4364.

[43] Kumar S., Chen W., Liu Z., S. Ji,2016, Effects of solar and geomagnetic activity on the occurrence of equatorial plasma

bubbles over Hong Kong, J. Geophys. Res. Space Phys. 121, 9164-9178.

[44] Tsunoda R.T., 1985. Control of the seasonal and longitudinal occurrence of equatorial scintillations by the longitudinal gradient in integrated E-region Pedersen conductivity, J. Geophys. Res. 90(A1), 447-456.

[45] Yeboah E.A., Paulino I., Medeiros A.F., Buriti R.A., Paulino A.R., Essien P.,S.O. Lomotey, H. Takahashi, C.M., 2019. Wrasse: Seasonal variation of plasma bubbles during solar cycle 23-24 over the Brazilian equatorial region, Advance in Space Res. 64 (7), 1365-1374.

[46] Valladares C.E., Villalobos J., Sheehan R., Hagan M.P. , 2004. Latitudinal extension of low-latitude scintillations measured with a network of GPS receivers, Ann. Geophys. 22(9), 3155-3175.

[47] Klobuchar J.A., Anderson D.N., Doherty P.H., 1991. Model studies of the latitudinal extent of the equatorial anomaly during equinoctial conditions, Radio Sci. 26(4), 1025-1047.

[48] Yeh K.C., Soicher H., Liu C.H., Bonelli E., 1979. Ionospheric bubbles observed by the Faraday rotation method at Natal, Brazil: Geophys. Res. Lett. 6(6), 473-475.

All © 2023 are reserved by International Journal of Advanced Science and Engineering. This Journal is licensed under a Creative Commons Attribution-Non Commercial-ShareAlike 3.0 Unported License.